Progress In Electromagnetics Research, PIER 20, 153–178, 1998

THE COMBINED EFFECTS OF CHIRAL OPERATION IN MULTILAYERED BIANISOTROPIC SUBSTRATES

W. Y. Yin, G. H. Nan, and I. Wolff

Department of Electrical Engineering
Duisburg University
47048 Duisburg, Germany

1. INTRODUCTION

In the past few years, complex linear materials have gained much and increasing attention in electromagnetic community, and among these bianisotropic materials must be mentioned [1]. Bianisotropic linear materials are characterized by four independent constitutive tensors, and till now significant theoretical research progress has been achieved concerning the electromagnetic characteristics and potential applications of some bianisotropic materials. For instance, the dyadic Green's function theory for source radiation and wave propagation in uniaxial and helicoidal bianisotropic media [2–8], wave reflection and transmission properties of multilayered bianisotropic slabs and their potential applications for making novel non-reflection coatings and filters [9–15], the guided hybrid mode features in some bianisotropic waveguides [16–24], the dispersion characteristics of bianisotropic microstrip transmission lines and the effects of bianisotropic substrate and su-

perstrate on the radiation of sources [25–28], the scattering from some particular bianisotropic objects [29–31], the edge effect in bianisotropic region [32, 33], and the macroscopic properties of bianisotropic mixtures as well as experimental investigations on the effective constitutive parameters of uniaxial bianisotropic composites [34–39], et al. In these studies the authors usually pay attention to the diverse chiral effects in bianisotropic media. However, it should be emphasized that, in spite of that both theoretical and experimental progress has been made on the electromagnetic characteristics of bianisotropic materials recently, there still remain many unsolved problems for further exploration.

It is known that the exponential matrix technique in spectral domain has often been utilized for investigating the interaction of electromagnetic waves with bi(an)isotropic media [3]. To some degree speaking, such a technique is efficient and powerful to deal with most linear complex materials, and it has been employed in the author's previous study and improved more recently [14, 28]. In this contribution, our attention is concentrated on the effects of chiral operation on the radiation characteristics of a dipole antenna placed on some grounded multilayered bianisotropic substrates, and this chiral operation is realized by stacking up a certain number of bianisotropic biaxial chiral plates in a way of the consecutive principal axes of four constitutive tensors $\left[c^{(i)}\right]$ $(c = \varepsilon, \mu, \xi_e, \xi_m)$ describing either right- or left-handed spirality, or ranging the orientation of biasing magnetic field in the right- or left-handed spirality in Faraday chiral plates. The bianisotropic chiral substrates possessing such structural features can be regarded as the typical cases of helicoidal bianisotropic media [7–12]. In the following sections the mathematical treatment is based on the exponential matrix technique in spectral domain, and the motivation for this study is not only of academic importance, but also essential for the potential applications of bianisotropic media.

2. THE GEOMETRY OF THE PROBLEM

The geometry of a grounded multilayered bianisotropic substrate is shown in Fig. 1, in which an elementary dipole antenna $J(R')$ is placed at the interface $z = 0$ along the x-direction, and the thickness of each layer is denoted by $d^{(1)}, \cdots, d^{(i)}, \left(\left|D^{(i)} - D^{(i-l)}\right|\right), \cdots, d_N$. Evidently, this structure is two-dimensional and homogeneous in the y-direction.

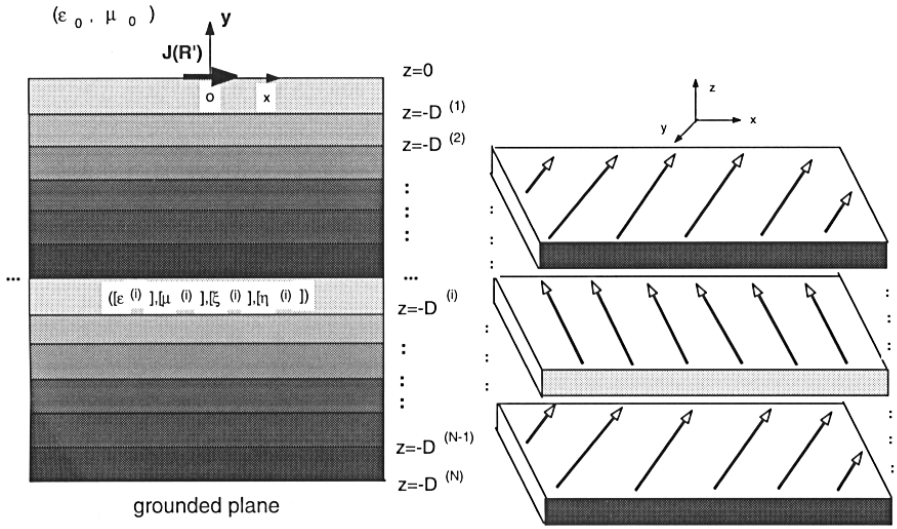

(a) (b)

Figure 1. The geometry of a grounded multilayered bianisotropic substrate. (a) cross-section (b) the orientations of the principal axes of constitutive tensors or the biasing magnetic field

The constitutive characteristics of each bianisotropic plate ($i = 1, \cdots, N$) in an appropriate frequency range can be described by:

$$\overline{D}^{(i)} = \varepsilon_0 \left[\varepsilon^{(i)}\right] \overline{E}^{(i)} + \sqrt{\mu_0 \varepsilon_0} \left[\xi^{(i)}\right] \overline{H}^{(i)} \tag{1a}$$

$$\overline{B}^{(i)} = \mu_0 \left[\mu^{(i)}\right] \overline{H}^{(i)} + \sqrt{\mu_0 \varepsilon_0} \left[\eta^{(i)}\right] \overline{E}^{(i)} \tag{1b}$$

where $\left[\varepsilon^{(i)}\right]$, $\left[\mu^{(i)}\right]$, $\left[\xi^{(i)}\right]$, and $\left[\eta^{(i)}\right]$ are relative permittivity, permeability, and cross coupling tensors of the ith layer, respectively. The time dependence e^{jwt} is assumed and suppressed throughout this paper. With respect to the above Cartesian coordinate system in Fig. 1, the four constitutive tensors of bianisotropic chiral plates in (1) should

take the following 3×3 matrix forms:

$$\left[\varepsilon^{(i)}\right] = \begin{bmatrix} \varepsilon_{xx}^{(i)} & \varepsilon_{xy}^{(i)} & 0 \\ \varepsilon_{yx}^{(i)} & \varepsilon_{yy}^{(i)} & 0 \\ 0 & 0 & \varepsilon_{zz}^{(i)} \end{bmatrix}, \quad \left[\mu^{(i)}\right] = \begin{bmatrix} \mu_{xx}^{(i)} & \mu_{xy}^{(i)} & 0 \\ \mu_{yx}^{(i)} & \mu_{yy}^{(i)} & 0 \\ 0 & 0 & \mu_{zz}^{(i)} \end{bmatrix}, \quad (2a, b)$$

$$\left[\xi^{(i)}\right] = \begin{bmatrix} \xi_{xx}^{(i)} & \xi_{xy}^{(i)} & 0 \\ \xi_{yx}^{(i)} & \xi_{yy}^{(i)} & 0 \\ 0 & 0 & \xi_{zz}^{(i)} \end{bmatrix}, \quad \left[\eta^{(i)}\right] = \begin{bmatrix} \eta_{xx}^{(i)} & \eta_{xy}^{(i)} & 0 \\ \eta_{yx}^{(i)} & \eta_{yy}^{(i)} & 0 \\ 0 & 0 & \eta_{zz}^{(i)} \end{bmatrix}, \quad (2c, d)$$

and

$$\begin{aligned}
\varepsilon_{xx}^{(i)} =& \varepsilon_{x}^{(i)} \cos^2 \theta_{e}^{(i)} + \varepsilon_{y}^{(i)} \sin^2 \theta_{e}^{(i)}, \\
\varepsilon_{xy}^{(i)} =& \varepsilon_{yx}^{(i)} = (\varepsilon_{y}^{(i)} - \varepsilon_{x}^{(i)}) \sin \theta_{e}^{(i)} \cos \theta_{e}^{(i)}, \\
\varepsilon_{yy}^{(i)} =& \varepsilon_{x}^{(i)} \sin^2 \theta_{e}^{(i)} + \varepsilon_{y}^{(i)} \cos^2 \theta_{e}^{(i)}, \\
\varepsilon_{zz}^{(i)} =& \varepsilon_{z}^{(i)}, \\
\mu_{xx}^{(i)} =& \mu_{x}^{(i)} \cos^2 \theta_{m}^{(i)} + \mu_{y}^{(i)} \sin^2 \theta_{m}^{(i)}, \\
\mu_{xy}^{(i)} =& \mu_{yx}^{(i)} = (\mu_{y}^{(i)} - \mu_{x}^{(i)}) \sin \theta_{m}^{(i)} \cos \theta_{m}^{(i)}, \\
\mu_{yy}^{(i)} =& \mu_{x}^{(i)} \sin^2 \theta_{m}^{(i)} + \mu_{y}^{(i)} \cos^2 \theta_{m}^{(i)}, \\
\mu_{zz}^{(i)} =& \mu_{z}^{(i)}, \\
\xi_{xx}^{(i)} =& \xi_{x}^{(i)} \cos^2 \theta_{em}^{(i)} + \xi_{y}^{(i)} \sin^2 \theta_{em}^{(i)}, \\
\xi_{xy}^{(i)} =& \xi_{yx}^{(i)} = (\xi_{y}^{(i)} - \xi_{x}^{(i)}) \sin \theta_{em}^{(i)} \cos \theta_{em}^{(i)}, \\
\xi_{yy}^{(i)} =& \xi_{x}^{(i)} \sin^2 \theta_{em}^{(i)} + \xi_{y}^{(i)} \cos^2 \theta_{em}^{(i)}, \\
\xi_{zz}^{(i)} =& \xi_{z}^{(i)}, \\
\eta_{xx}^{(i)} =& \eta_{x}^{(i)} \cos^2 \theta_{me}^{(i)} + \eta_{y}^{(i)} \sin^2 \theta_{me}^{(i)}, \\
\eta_{xy}^{(i)} =& \eta_{yx}^{(i)} = (\eta_{y}^{(i)} - \eta_{x}^{(i)}) \sin \theta_{me}^{(i)} \cos \theta_{me}^{(i)}, \\
\eta_{yy}^{(i)} =& \eta_{x}^{(i)} \sin^2 \theta_{me}^{(i)} + \eta_{y}^{(i)} \cos^2 \theta_{me}^{(i)}, \\
\eta_{zz}^{(i)} =& \eta_{z}^{(i)}, \qquad (2e)
\end{aligned}$$

where $\theta_e^{(i)}, \theta_m^{(i)}, \theta_{em}^{(i)}$ and $\theta_{me}^{(i)} \in [0°, \pm 360°]$ are the orientation angles of the principal axes of $\left[\varepsilon^{(i)}\right]$, $\left[\mu^{(i)}\right]$, $\left[\xi^{(i)}\right]$, and $\left[\eta^{(i)}\right]$ with respect to the x-direction in x-y plane, respectively. The orientations of axes should be in a right- or left-handed ($+$: right; $-$: left) spirality and periodically in the z-direction. In (2) $\theta_e^{(i)} = \theta_m^{(i)} = \theta_{em}^{(i)} = \theta_{me}^{(i)}$ just stands

for the double chiralities case in bianisotropic chiral substrates, and especially, when $\left[\xi^{(i)}\right] = \left[\eta^{(i)}\right] = 0$ reduces to the special case of multilayered chiral arrangement of a uniaxial or biaxial model [40]. On the other hand, when the thickness of each layer $d^{(i)} \ll \lambda$ (the operating wavelength) and $c_x^{(i)} = c_x^{(i-1)}, c_y^{(i)} = c_y^{(i-1)}, c_z^{(i)} = c_z^{(i-1)} (c = \varepsilon, \mu, \xi, \eta)$, the stepwise variation will appear to be continuous, and under such circumstances the above structure can then be thought of as a smoothly non-homogeneous medium with helicoidally varying properties [6–12]. Physically, all constitutive parameters of the bianisotropic substrate above should be a function of the operating frequency and must be within the confines of a realizable range, and [15]

$$j \begin{bmatrix} \left[\varepsilon^{(i)}\right] - \left[\varepsilon^{(i)}\right]^{\otimes} & \left[\eta^{(i)}\right] - \left[\eta^{(i)}\right]^{\otimes} \\ \left[\xi^{(i)}\right] - \left[\xi^{(i)}\right]^{\otimes} & \left[\mu^{(i)}\right] - \left[\mu^{(i)}\right]^{\otimes} \end{bmatrix}$$

is positive semi-definite, here the superscript $\otimes$ denotes the double operation of transpose and complex conjugation. It is known that Faraday chiral composites (i.e., chiroferrites and chiroplasmas) are an important group of bianisotropic materials, and in such composites both gyrotropy and chirality can be introduced simultaneously [24, 27–30, 38, 39, 41, 42]. Correspondingly, four constitutive tensors in (1) for chiroferrites can be written as

$$\left[\varepsilon^{(i)}\right] = \varepsilon^{(i)}\overline{\overline{I}}, \left[\xi^{(i)}\right] = \left[\eta^{(i)}\right]^{*} = j\kappa^{(i)}\overline{\overline{I}}, \quad \left[\mu^{(i)}\right] = \begin{bmatrix} \mu_{xx}^{(i)} & \mu_{xy}^{(i)} & \mu_{xz}^{(i)} \\ \mu_{yx}^{(i)} & \mu_{yy}^{(i)} & \mu_{yz}^{(i)} \\ \mu_{zx}^{(i)} & \mu_{zy}^{(i)} & \mu_{zz}^{(i)} \end{bmatrix}, \quad i = 1, 2, \cdots, N \quad (3a)$$

and here chiroferrites are biased by static magnetic fields $\overline{H}_0^{(i)}$ of arbitrary orientation $(\varphi_0^{(i)}, \theta_0^{(i)})$ [28], i.e.,

$$\begin{aligned}
\mu_{xx}^{(i)}(\omega) =& \mu^{(i)}(\omega) + [1 - \mu^{(i)}(\omega)] \sin^2 \theta_0^{(i)} \cos^2 \varphi_0^{(i)}, \\
\mu_{xy}^{(i)}(\omega) =& [1 - \mu^{(i)}(\omega)] \sin \varphi_0^{(i)} \cos \varphi_0^{(i)} \sin^2 \theta_0^{(i)} - j\kappa_c^{(i)} \cos \theta_0^{(i)}, \\
\mu_{xz}^{(i)}(\omega) =& j\kappa_c^{(i)} \sin \varphi_0^{(i)} \sin \theta_0^{(i)} + [1 - \mu^{(i)}(\omega)] \sin \theta_0^{(i)} \cos \theta_0^{(i)} \cos \varphi_0^{(i)}, \\
\mu_{yx}^{(i)}(\omega) =& [1 - \mu^{(i)}(\omega)] \sin \varphi_0^{(i)} \cos \varphi_0^{(i)} \sin^2 \theta_0^{(i)} + j\kappa_c^{(i)} \cos \theta_0^{(i)}, \\
\mu_{yy}^{(i)}(\omega) =& \mu^{(i)}(\omega) + [1 - \mu^{(i)}(\omega)] \sin^2 \theta_0^{(i)} \sin^2 \varphi_0^{(i)},
\end{aligned}$$

$$\mu_{yz}^{(i)}(\omega) = -j\kappa_c^{(i)}\cos\varphi_0^{(i)}\sin\theta_0^{(i)} + [1-\mu^{(i)}(\omega)]\sin\theta_0^{(i)}\cos\theta_0^{(i)}\sin\varphi_0^{(i)},$$
$$\mu_{zx}^{(i)}(\omega) = -j\kappa_c^{(i)}\sin\varphi_0^{(i)}\sin\theta_0^{(i)} + [1-\mu^{(i)}(\omega)]\sin\theta_0^{(i)}\cos\theta_0^{(i)}\cos\varphi_0^{(i)},$$
$$\mu_{zy}^{(i)}(\omega) = j\kappa_c^{(i)}\cos\varphi_0^{(i)}\sin\theta_0^{(i)} + [1-\mu^{(i)}(\omega)]\sin\theta_0^{(i)}\cos\theta_0^{(i)}\sin\varphi_0^{(i)},$$
$$\mu_{zz}^{(i)}(\omega) = 1 - [1-\mu^{(i)}(\omega)]\sin^2\theta_0^{(i)},$$

$$\mu^{(i)}(\omega) = \mu_1^{(i)}(\omega) - j\mu_2^{(i)}(\omega), \quad \mu_1^{(i)}(\omega) = 1 + \frac{\omega_0^{(i)}\omega_m^{(i)}[{\omega_0^{(i)}}^2 - \omega^2(1-{\alpha_m^{(i)}}^2)]}{F_m^{(i)}},$$
$$\mu_2^{(i)}(\omega) = \frac{\omega\omega_m^{(i)}\alpha_m^{(i)}[{\omega_0^{(i)}}^2 + \omega^2(1+{\alpha_m^{(i)}}^2)]}{F_m^{(i)}},$$
$$\kappa_c^{(i)}(\omega) = \kappa_{c1}^{(i)}(\omega) - j\kappa_{c2}^{(i)}(\omega), \quad \kappa_{c1}^{(i)}(\omega) = -\frac{\omega\omega_m^{(i)}[{\omega_0^{(i)}}^2 - \omega^2(1+{\alpha_m^{(i)}}^2)]}{F_m^{(i)}},$$
$$\kappa_{c2}^{(i)} = -\frac{2\omega_m\omega_0^{(i)}\alpha_m^{(i)}\omega^2}{F_m^{(i)}}, \quad F_m^{(i)} = [{\omega_0^{(i)}}^2 - \omega^2(1+{\alpha_m^{(i)}}^2)]^2 + 4(\omega\omega_0^{(i)}\alpha_m^{(i)})^2,$$
$$\omega = |\gamma|H_0^{(i)}, \quad \omega_m^{(i)} = |\gamma|M_s^{(i)}, \tag{3b}$$

where $M_s^{(i)}$ is the saturation magnetization of the chiroferrite; γ, the gyromagnetic ratio ($= -2.21 \times 10^5\, rad\ m/C$); $\alpha_m^{(i)}$, the Landau damping coefficient and the loss is taken into account. Especially, when the orientation of $\overline{H}_0^{(i)}$ is in the right- or left-handed spirality for the given $\theta_0^{(i)}$ ($\varphi_0 \in (0^\circ, \pm 360^\circ)$), double chiralities are formed in the multilayered chiroferrite substrate. While for chiroplasmas,

$$\left[\mu^{(i)}\right] = \mu^{(i)}\overline{\overline{I}}, \left[\xi^{(i)}\right] = \left[\eta^{(i)}\right]^* = j\kappa^{(i)}\overline{\overline{I}}, \quad \left[\varepsilon^{(i)}\right] = \begin{bmatrix} \varepsilon_{xx}^{(i)} & \varepsilon_{xy}^{(i)} & \varepsilon_{xz}^{(i)} \\ \varepsilon_{yx}^{(i)} & \varepsilon_{yy}^{(i)} & \varepsilon_{yz}^{(i)} \\ \varepsilon_{zx}^{(i)} & \varepsilon_{zy}^{(i)} & \varepsilon_{zz}^{(i)} \end{bmatrix}, \tag{4a}$$

According to the related form of $\left[\varepsilon^{(i)}\right]$ in [43] and after the rotation of Cartesian coordinate system, we obtain

$$\varepsilon_{xx}^{(i)}(\omega) = \varepsilon_1^{(i)}(\omega) + [\varepsilon_2^{(i)}(\omega) - \varepsilon_1^{(i)}(\omega)]\sin^2\nu^{(i)}\cos^2\psi^{(i)},$$
$$\varepsilon_{xy}^{(i)}(\omega) = \{jg^{(i)}\sin\psi^{(i)} + [\varepsilon_2^{(i)}(\omega) - \varepsilon_1^{(i)}(\omega)]\cos\psi^{(i)}\cos\nu^{(i)}\}\sin\nu^{(i)},$$
$$\varepsilon_{xz}^{(i)}(\omega) = -ig^{(i)}(\omega)\cos\nu^{(i)} + [\varepsilon_2^{(i)}(\omega) - \varepsilon_1^{(i)}(\omega)]\sin\psi^{(i)}\cos\psi^{(i)}\sin^2\nu^{(i)},$$

$$
\begin{aligned}
\varepsilon_{yx}^{(i)}(\omega) =& \{-jg^{(i)} \sin\psi^{(i)} + [\varepsilon_2^{(i)}(\omega) - \varepsilon_1^{(i)}(\omega)] \cos\psi^{(i)} \cos\nu^{(i)}\} \sin\nu^{(i)},\\
\varepsilon_{yy}^{(i)}(\omega) =& \varepsilon_1^{(i)} \sin^2\nu^{(i)} + \varepsilon_2^{(i)}(\omega) \cos^2\nu^{(i)},\\
\varepsilon_{yz}^{(i)}(\omega) =& \{jg^{(i)} \cos\psi^{(i)} + [\varepsilon_2^{(i)}(\omega) - \varepsilon_1^{(i)}(\omega)] \sin\psi^{(i)} \cos\nu^{(i)}\} \sin\nu^{(i)},\\
\varepsilon_{zx}^{(i)}(\omega) =& ig^{(i)}(\omega) \cos\nu^{(i)} + [\varepsilon_2^{(i)}(\omega) - \varepsilon_1^{(i)}(\omega)] \sin\psi^{(i)} \cos\psi^{(i)} \sin^2\nu^{(i)},\\
\varepsilon_{zy}^{(i)}(\omega) =& \{-jg^{(i)} \cos\psi^{(i)} + [\varepsilon_2^{(i)}(\omega) - \varepsilon_1^{(i)}(\omega)] \sin\psi^{(i)} \cos\nu^{(i)}\} \sin\nu^{(i)},\\
\varepsilon_{zz}^{(i)}(\omega) =& \varepsilon_1^{(i)}(\omega) + [\varepsilon_2^{(i)}(\omega) - \varepsilon_1^{(i)}(\omega)] \sin^2\nu^{(i)} \sin^2\psi^{(i)},
\end{aligned} \tag{4b}
$$

and $\psi^{(i)}$ and $\nu^{(i)}$ are determined by the spherical angles, $\theta_0^{(i)}$ and $\varphi_0^{(i)}$ through

$$
\cos\psi^{(i)} = \frac{\sin\theta_0^{(i)} \cos\varphi_0^{(i)}}{\sqrt{\sin^2\theta_0^{(i)} \cos^2\varphi_0^{(i)} + \cos^2\theta_0^{(i)}}}, \quad \cos\nu^{(i)} = \sin\theta_0^{(i)} \sin\varphi_0^{(i)}, \tag{4c}
$$

where

$$
\begin{aligned}
\varepsilon_1^{(i)}(\omega) =& \varepsilon_s^{(i)} - \frac{{\omega_p^{(i)}}^2 (\omega - j\tau^{(i)^{-1}})}{\omega[(\omega - j\tau^{(i)^{-1}})^2 - {\omega_c^{(i)}}^2]}, \quad \varepsilon_2^{(i)}(\omega) = \varepsilon_s^{(i)} - \frac{{\omega_p^{(i)}}^2}{\omega(\omega - j\tau^{(i)^{-1}})},\\
g^{(i)}(\omega) =& -\frac{{\omega_p^{(i)}}^2 \omega_c^{(i)}}{\omega[(\omega - j\tau^{(i)^{-1}})^2 - {\omega_c^{(i)}}^2]},
\end{aligned} \tag{4d}
$$

and $\omega_p^{(i)} = \sqrt{(n^{(i)}e^2/\varepsilon_0 m^*)}$ represents the plasma frequency; $\omega_c^{(i)} = eB_0^{(i)}/m^*$, the cyclotron frequency; $n^{(i)}$, the carriers' concentration; e, the electron charge; m^*, the electron effective mass (kg) (i.e., 0.067 m_e for GaAs); m_e, the electron rest mass; $B_0^{(i)}$, the DC magnetizing field; $\varphi^{(j)}$, the orientation angle of $B_0^{(i)}$ in the x-y plane; $\tau^{(i)}$, the momentum relaxation time of the semiconductor material; and $\varepsilon_s^{(i)}$, the relative dielectric permittivity of the semiconductor. Evidently, when the external DC magnetic field $B_0^{(i)}$ in each layer of chiroplasma substrate take the same orientation as in chiroferrite, double chiralities can also be formed in the above multilayered substrate.

3. THE FAR FIELD DISTRIBUTIONS

Introducing the Fourier transform domain defined by

$$\widetilde{\psi}(k_x, k_y; z) = \int_{-\infty}^{+\infty}\int_{-\infty}^{+\infty} \psi(x, y; z) e^{j(k_x x + k_y y)} dx dy, \tag{5a}$$

$$\psi(x, y; z) = \int_{-\infty}^{+\infty}\int_{-\infty}^{+\infty} \widetilde{\psi}(k_x, k_y; z) e^{-j(k_x x + k_y y)} dk_x dk_y, \tag{5b}$$

into the following Maxwell's equations:

$$\nabla \times \overline{H}^{(i)} = j\omega\{\varepsilon_0[\varepsilon^{(i)}]\overline{E}^{(i)} + \sqrt{\mu_0\varepsilon_0}[\xi^{(i)}]\overline{H}^{(i)}\}, \tag{6a}$$

$$\nabla \times \overline{E}^{(i)} = -j\omega\{\mu_0[\mu^{(i)}]\overline{H}^{(i)} + \sqrt{\mu_0\varepsilon_0}[\eta^{(i)}]\overline{E}^{(i)}\}, \tag{6b}$$

and following a similar procedure used in [28], the transverse field components in each layer of multilayered bianisotropic slabs can be expressed as:

$$\frac{d}{dz}\begin{bmatrix} \widetilde{E}_x^{(i)}(k_x, k_y; z) \\ \widetilde{E}_y^{(i)}(k_x, k_y; z) \\ \widetilde{H}_x^{(i)}(k_x, k_y; z) \\ \widetilde{H}_y^{(i)}(k_x, k_y; z) \end{bmatrix} = \begin{bmatrix} p_{11}^{(i)} & p_{12}^{(i)} & p_{13}^{(i)} & p_{14}^{(i)} \\ p_{21}^{(i)} & p_{22}^{(i)} & p_{23}^{(i)} & p_{24}^{(i)} \\ p_{31}^{(i)} & p_{32}^{(i)} & p_{33}^{(i)} & p_{34}^{(i)} \\ p_{41}^{(i)} & p_{42}^{(i)} & p_{43}^{(i)} & p_{44}^{(i)} \end{bmatrix} \begin{bmatrix} \widetilde{E}_x^{(i)}(k_x, k_y; z) \\ \widetilde{E}_y^{(i)}(k_x, k_y; z) \\ \widetilde{H}_x^{(i)}(k_x, k_y; z) \\ \widetilde{H}_y^{(i)}(k_x, k_y; z) \end{bmatrix}. \tag{7}$$

where $p_{11}^{(i)}$ - $p_{44}^{(i)}$ developed in [28] have some printing errors, and their exact expressions are presented in APPENDIX 1 for the multilayered case. Furthermore, the general solution to the vector differential Eq.(7) can be found:

$$\begin{bmatrix} \widetilde{E}_x^{(i)}(k_x, k_y; z) \\ \widetilde{E}_y^{(i)}(k_x, k_y; z) \\ \widetilde{H}_x^{(i)}(k_x, k_y; z) \\ \widetilde{H}_y^{(i)}(k_x, k_y; z) \end{bmatrix} = \begin{bmatrix} T_{11}^{(i)}(z) & T_{12}^{(i)}(z) & T_{13}^{(i)}(z) & T_{14}^{(i)}(z) \\ T_{21}^{(i)}(z) & T_{22}^{(i)}(z) & T_{23}^{(i)}(z) & T_{24}^{(i)}(z) \\ T_{31}^{(i)}(z) & T_{32}^{(i)}(z) & T_{33}^{(i)}(z) & T_{34}^{(i)}(z) \\ T_{41}^{(i)}(z) & T_{42}^{(i)}(z) & T_{43}^{(i)}(z) & T_{44}^{(i)}(z) \end{bmatrix} \begin{bmatrix} \widetilde{E}_x^{(i)}(k_x, k_y; 0) \\ \widetilde{E}_y^{(i)}(k_x, k_y; 0) \\ \widetilde{H}_x^{(i)}(k_x, k_y; 0) \\ \widetilde{H}_y^{(i)}(k_x, k_y; 0) \end{bmatrix} \tag{8}$$

and here the matrix $[T^{(i)}(z)]_{4\times4}$ is to relate the tangential electromagnetic fields at the surface z to the tangential fields at the surface $z = 0$ within the ith layer, and in each layer $[T^{(i)}(z)]_{4\times4}$ is calculated in the exponential matrix form by means of Cayley-Hamilton theorem combined with Muller's root-finding technique. While the total transmission matrix $[T(-D^{(N)})]_{4\times4}$ relating the boundary condition at $z = 0$ to that of $z = -D^{(N)}$ is calculated from $[T^{(i)}(z)]_{4\times4}$ $(i = 1, \cdots, N)$ in the form of serial matrix. At some extreme cases the above procedure breaks down, however, such cases will not be met here.

Under the excitation of a dipole antenna on the multilayered bianisotropic chiral substrate, the far field distributions in the air region $(z > 0)$ can be derived using the saddle-point method, i.e., [3]

$$E_\theta = j\frac{2\pi\widetilde{\psi}_1}{R\sin\theta}e^{-jk_0R}, \quad E_\varphi = -j\frac{2\pi\widetilde{\psi}_2}{R\tan\theta}e^{-jk_0R} \tag{9a, b}$$

where

$$\widetilde{\psi}_1 = k_x\widetilde{E}_x^{(0)}(k_x, k_y, 0) + k_y\widetilde{E}_y^{(0)}(k_x, k_y, 0), \tag{9c}$$

$$\widetilde{\psi}_2 = k_y\widetilde{E}_x^{(0)}(k_x, k_y, 0) - k_x\widetilde{E}_y^{(0)}(k_x, k_y, 0), \tag{9d}$$

and $k_0 = \omega\sqrt{\mu_0\varepsilon_0}$.

4. NUMERICAL RESULTS

Based on the mathematical formulation presented in the previous section, computer codes have been developed for examining the effects of chiral operation in a multilayered bianisotropic substrate on the radiation characteristics of a dipole antenna on the top surface $z = 0$. The material parameters used for calculations are related to parameters used in the literature, and the losses of the materials are neglected here so that the attenuation by the bianisotropic substrates can not mask effects produced by chiral operation. In addition, it should be emphasized that the developed computer codes have been checked at first and all figures in [28, 44] have been reproduced under the corresponding conditions.

At first, the normalized far-field patterns of a dipole antenna on a grounded 13-layer bianisotropic biaxial substrate are examined with respect to different chiral operations. The thickness of each layer is assumed to be $d^{(i)} = 0.2\,\text{mm}$ $(i = 1, \cdots, 13)$ and the operating frequency is $f = 17.25$ GHz.

In Fig. 2, both co- and cross-polarized components of the far-field are symmetrical to the direction $\theta = \theta_m = 0^\circ$. Here θ_m is the main beam direction and its definition is the same as in [28, 44] (i.e., the beam due to the co-polarized component of the electric field only, and for x-directed dipole in the $\varphi = 90^\circ$ plane this implies E_φ component). Since the axes of the four constitutive tensors $\left[c^{(i)}\right]$ $(c = \varepsilon, \mu, \xi, \eta)$ in case (a) are chosen to be in the same direction $(\theta_e^{(i)} = \theta_m^{(i)} = \theta_{em}^{(i)} = \theta_{me}^{(i)} = 45^\circ)$ in the 13-layer substrate, it is just equivalent to the case of an one-layer substrate. In addition, the cross coupling tensors $\left[\xi^{(i)}\right]$ and $\left[\eta^{(i)}\right]$ in Fig. 2(a) are supposed to be in the uniaxial form, i.e., $\xi_x^{(i)} = \xi_y^{(i)} = \eta_x^{(i)^*} = \eta_y^{(i)^*}$. In Fig. 2(b), the orientation of the axes of $\left[c^{(i)}\right]$ $(c = \varepsilon, \mu, \xi, \eta)$ are chosen to be the same and in the right- or left-handed spirality, respectively. The phase difference between adjacent layers in the substrate are assumed to be: $\Delta\theta_{e,m,em,me}^{(i)} = \theta_{e,m,em,me}^{(i+1)} - \theta_{e,m,em,me}^{(i)} = \pm 45^\circ$. So double chiralities are introduced in the 13-layer substrate, but $\left[\xi^{(i)}\right]$ and $\left[\eta^{(i)}\right]$ are also of uniaxial form. It is obvious that the cross-polarized component E_θ in the $\varphi = 90^\circ$ plane is nearly zero $(E_\theta \ll E_\varphi)$. However, in the $\varphi = 60^\circ(120^\circ)$ plane the magnitude of E_θ is comparable to E_φ (Fig. 3(c)). Numerical calculation for case $\Delta\theta_{e,m,em,me}^{(i)} = \pm 60^\circ$ has also been carried out and a similar conclusion can be obtained. More generally, in Fig. 3(d) the orientation of the axes of $\left[c^{(i)}\right]$ $(c = \varepsilon, \mu, \xi, \eta)$ is in the right- and left-handed spiralities $(\left|\Delta\theta_{e,m,em,me}^{(i)}\right| = 45^\circ)$, respectively, but the axis of $\left[\mu^{(i)}\right]$ $(\left[\eta^{(i)}\right])$ is not in concordance with that of $\left[\varepsilon^{(i)}\right]$ $(\left[\xi^{(i)}\right])$. Since $\xi_x^{(i)}(\eta_x^{(i)^*}) \neq \xi_y^{(i)}(\eta_y^{(i)^*}) \neq \xi_z^{(i)}(\eta_z^{(i)^*})$, $\left[\xi^{(i)}\right]$ and $\left[\eta^{(i)}\right]$ are not of uniaxial form, and they take the general form as shown as in (2). The above numerical results show that for co-and cross-polarized far-field components:

$$\begin{aligned} & E_\varphi(\varphi, \pm\theta_{e,m,em,me}^{(i)}, \pm\xi_{x,y,z}^{(i)}, \pm\eta_{x,y,z}^{(i)}) \\ = & E_\varphi(180^\circ - \varphi, \mp\theta_{e,m,em,me}^{(i)}, \mp\xi_{x,y,z}^{(i)}, \mp\eta_{x,y,z}^{(i)}), \end{aligned} \tag{10a}$$

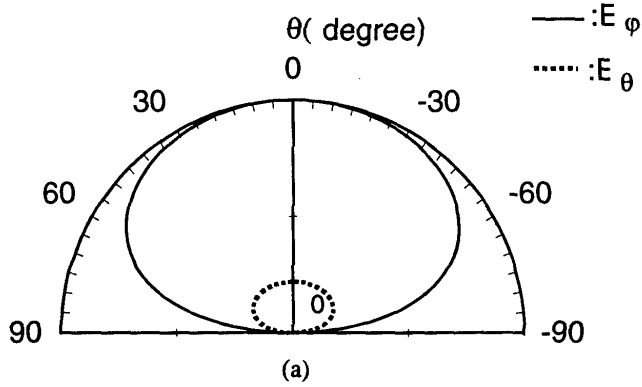

(a) $\varphi = 90°$, $\varepsilon_x^{(i)} = 2.0$, $\varepsilon_y^{(i)} = 2.35$, $\varepsilon_z^{(i)} = 3.5$, $\mu_x^{(i)} = 2.75$, $\mu_y^{(i)} = 2.25$, $\mu_z^{(i)} = 5.0$, $\xi_x^{(i)} = \xi_y^{(i)} = \eta_x^{(i)^*} = \eta_y^{(i)^*} = j0.2$, $\xi_z^{(i)} = \eta_z^{(i)^*} = j0.3$ (*: the complex conjugation), $\theta_e^{(i)} = \theta_m^{(i)} = \theta_{em}^{(i)} = \theta_{me}^{(i)} = 45°$.

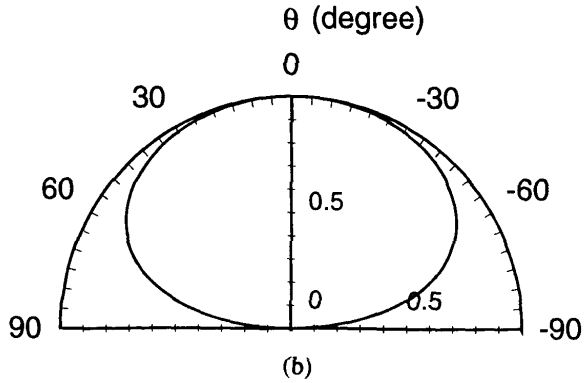

(b) The parameters are the same as in (a), except that $\xi_x^{(i)} = \xi_y^{(i)} = \eta_x^{(i)^*} = \eta_y^{(i)^*} = \pm j0.2$, $\xi_z^{(i)} = \eta_z^{(i)^*} = \pm j0.3$, $\theta_e^{(i)} = \theta_m^{(i)} = \theta_{em}^{(i)} = \theta_{me}^{(i)} = 0°/\pm 45°/\pm 90°/\pm 135°/\pm 180°/\pm 225°/\pm 270°/\pm 315°/\pm 360°/\pm 45°/\pm 90°/\pm 135°/\pm 180°$.

Figure 2. Normalized radiation pattern for a dipole antenna on a 13-layer bianisotropic chiral substrate. $f = 17.25\,\text{GHz}$, $d^{(i)} = 0.2\,\text{mm}$, $i = 1, \cdots, 13$, and

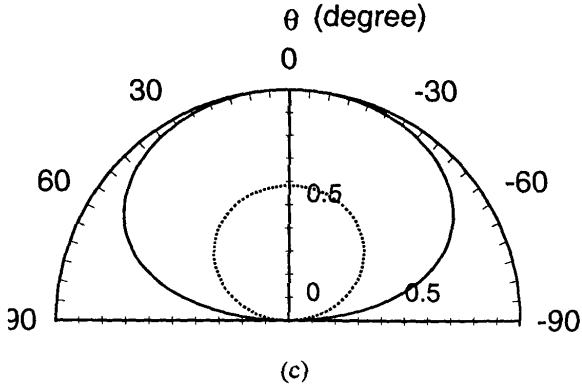

(c)

(c) The parameters are the same as (b), except that $\varphi = 60°(120°)$.

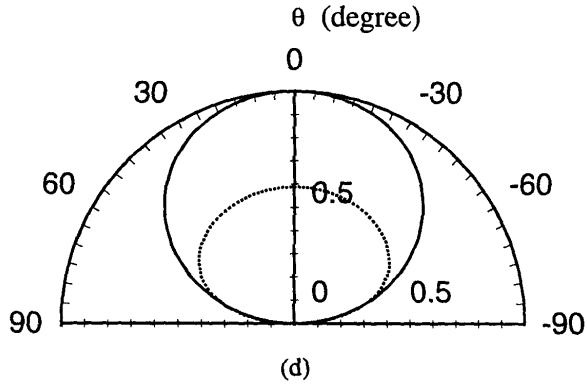

(d)

(d) $\varphi = 30°(150°)$, $\varepsilon_x^{(i)} = 2.0$, $\varepsilon_y^{(i)} = 2.35$, $\varepsilon_z^{(i)} = 3.5$, $\mu_x^{(i)} = 2.75$, $\mu_y^{(i)} = 2.25$, $\mu_z^{(i)} = 5.0$, $\xi_x^{(i)} = \eta_x^{(i)^*} = \pm j0.1$, $\xi_y^{(i)} = \eta_y^{(i)^*} = \pm j0.2$, $\xi_z^{(i)} = \eta_z^{(i)^*} = \pm j0.3$, $\theta_e^{(i)} = \theta_{em}^{(i)} = -\theta_m^{(i)} = -\theta_{me}^{(i)} = 0°/\pm 45°/\pm 90°/\pm 135°/\pm 180°/\pm 225°/\pm 270°/\pm 315°/\pm 360°/\pm 45°/\pm 90°/\pm 135°/\pm 180°$.

Figure 2. Normalized radiation pattern for a dipole antenna on a 13-layer bianisotropic chiral substrate. $f = 17.25\,\text{GHz}$, $d^{(i)} = 0.2\,\text{mm}$, $i = 1, \cdots, 13$, and

$$E_\theta(\varphi, \pm\theta^{(i)}_{e,m,em,me}, \pm\xi^{(i)}_{x,y,z}, \pm\eta^{(i)}_{x,y,z})$$
$$= E_\theta(180^\circ - \varphi, \mp\theta^{(i)}_{e,m,em,me}, \mp\xi^{(i)}_{x,y,z}, \mp\eta^{(i)}_{x,y,z}), \qquad (10b)$$

This means that for any source excitation and in the given directions (θ, φ) and $(\theta, 180^\circ - \varphi)$ either co- or cross-polarized components of the radiation field are equal if such kind of chiral operation is performed: reversing the spiral orientation of the axes of $\left[c^{(i)}\right]$ $(c = \varepsilon, \mu, \xi, \eta)$ and the sign of the cross coupling tensors $\left[\xi^{(i)}\right]$ and $\left[\eta^{(i)}\right]$ (i.e., the signs of chiralities parameters) simultaneously. It must be pointed out that (10) has no relation to the operating frequency, the source place, or the geometrical size of bianisotropic chiral substrate (i.e., the layer number and thickness of each layer). (10) is also true for the bianisotropic chiral superstrate-substrate structure or the infinite coupled dipole-array excitation [45], but indeed not true when $\left[\xi^{(i)}\right] = \left[\eta^{(i)}\right] = 0$. On the other hand, various numerical tests prove that both operating frequency and orientation angle of the axes of $\left[c^{(i)}\right]$ has no effect on the main beam direction, and θ_m is always kept in the direction of 0° for the above constitutive model of the bianisotropic biaxial substrate.

Fig. 3 demonstrates the normalized far-field patterns of a dipole antenna on a 13-layer chiroferrite substrate, and the thickness of each layer of the substrate is assumed to be $d^{(i)} = 0.2\,\text{mm}$. The operating frequency is $f = 17.25\,\text{GHz}$, the permittivity tensors of chiroferrites $\left[\varepsilon^{(i)}\right] = 12.6\overline{\overline{I}}$, and the Landau damping effect is not considered here.

In Fig. 3(a), since the biased static magnetic fields $\overline{H}_0^{(i)}$ take the same orientation in x-y plane $(\theta_0^{(i)} = 90^\circ, \varphi_0^{(i)} = 45^\circ)$ in each layer of substrates, it is just an one-layer substrate case and only one chirality is introduced here. While in Figs. 3(b)(c) double chiralities are introduced: one is caused by the right-handed spiral orientation of the biasing $\overline{H}_0^{(i)}$ denoting by the azimuthal bias angle $\{+\varphi_0^{(i)}\}$ and the other is due to the presentation of $\kappa^{(i)}$. Comparing (c) with (b) it is obvious that not only the relative level of E_φ and E_θ but also the main beam direction θ_m is changed with increasing $\kappa^{(i)}$, and θ_m is changed just nearly from -47.5° to $+47.5^\circ$. In Figs. 3(d)(e), there also exist double chiralities: the positive sign of $\kappa^{(i)}$ corresponds to the azimuthal bias angles $\{+\varphi_0^{(i)}\}$ representing the right-handed orientation of $\overline{H}_0^{(i)}$, and the negative sign of $\kappa^{(i)}$ corresponds to the left-handed orientation. In addition, in case (e) $\theta_0^{(i)}$ is chosen to be 60° and 120°, respectively, so the orientation of $\overline{H}_0^{(i)}$ takes the general

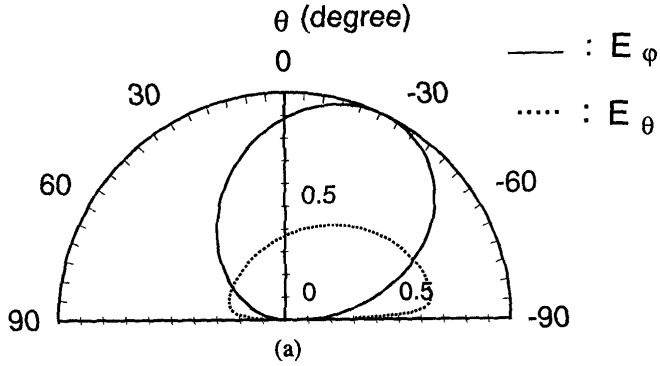

(a) $\varphi = 90°$, $M_s^{(i)}\mu_0 = 0.275$, $\omega_0^{(i)}/\omega_m^{(i)} = 2.0$, $\kappa^{(i)} = 0.4$, $\theta_0^{(i)} = 90°$, $\varphi_0^{(i)} = 45°$.

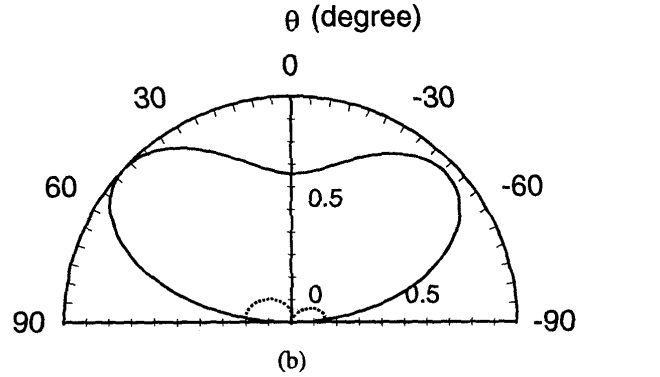

(b) $\varphi = 90°$, $M_s^{(i)}\mu_0 = 0.275$, $\omega_0^{(i)}/\omega_m^{(i)} = 0.2$, $\kappa^{(i)} = 0.1$, $\theta_0^{(i)} = 90°$.

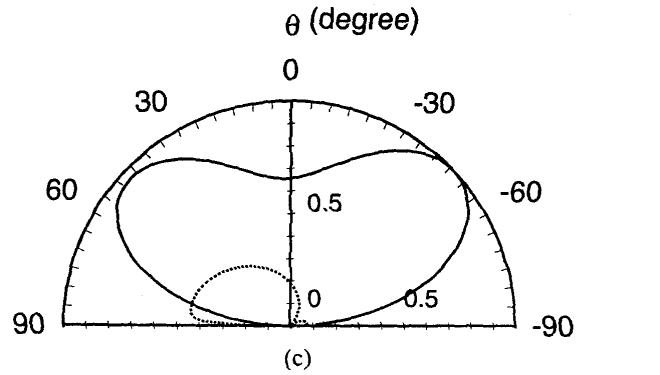

(c) The parameters are the same as (b), except that $\kappa^{(i)} = 0.5$.

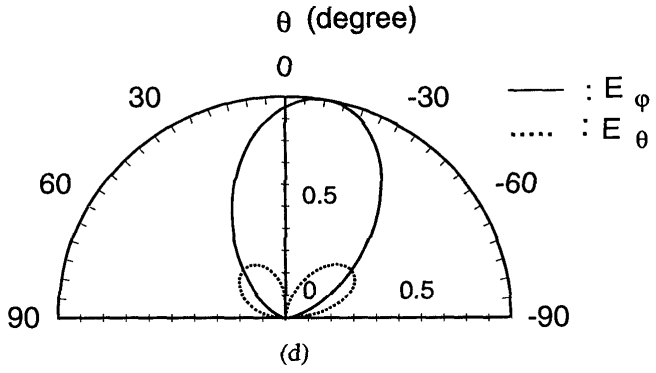

(d) $\varphi = 90°,\ M_s^{(i)}\mu_0 = 0.275,\ \omega_0^{(i)}/\omega_m^{(i)} = 2.0,\ \kappa^{(i)} = \pm 0.4,\ \theta_0^{(i)} = 90°,\ \varphi_0^{(i)} = 0°/\pm 60°/\pm 120°/\pm 180°/\pm 240°/\pm 300°/\pm 360°/\pm 60°/\pm 120°/\pm 180°/\pm 240°/\pm 300°/\pm 360°$.

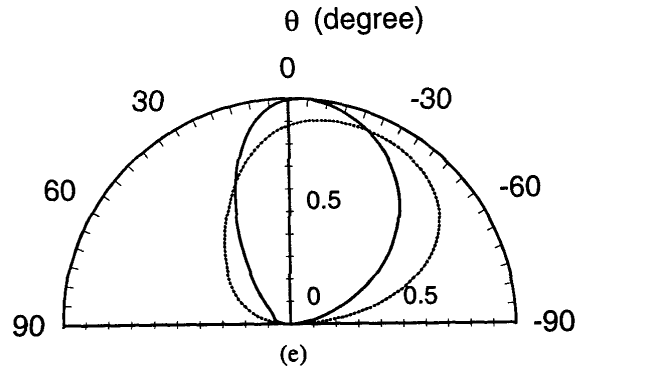

(e) $\varphi = 35°(145°),\ M_s^{(i)}\mu_0 = 0.275,\ \omega_0^{(i)}/\omega_m^{(i)} = 2.0,\ \kappa^{(i)} = \pm 0.4,\ \theta_0^{(i)} = 60°(120°),\ \varphi_0^{(i)} = 0°/\pm 60°/\pm 120°/\pm 180°/\pm 240°/\pm 300°/\pm 360°/\pm 60°/\pm 120°/\pm 180°/\pm 240°/\pm 300°/\pm 360°$.

Figure 3. Normalized radiation pattern for a dipole antenna on a 13-layer chiroferrite substrate. $f = 17.25\,\mathrm{GHz},\ \left[\varepsilon^{(i)}\right] = 12.6\overline{\overline{I}},\ d^{(i)} = 0.2\,\mathrm{mm},\ \alpha_m^{(i)} = 0,\ i = 1, \cdots, 13,$ and

right- and left-handed spiralities. It is interesting to note that:

$$E_\varphi(\varphi, \theta_0^{(i)}, \pm\varphi_0^{(i)}, \pm\kappa^{(i)}) = E_\varphi(180^\circ - \varphi, 180^\circ - \theta_0^{(i)}, \mp\varphi_0^{(i)}, \mp\kappa^{(i)}), \quad (11a)$$

$$E_\theta(\varphi, \theta_0^{(i)}, \pm\varphi_0^{(i)}, \pm\kappa^{(i)}) = E_\theta(180^\circ - \varphi, 180^\circ - \theta_0^{(i)}, \mp\varphi_0^{(i)}, \mp\kappa^{(i)}), \quad (11b)$$

This indicates that in the directions of (θ, φ) and $(\theta, 180^\circ - \varphi)$, E_φ and E_θ do not change for any source excitation if we take two chiral operations: reversing the spiral orientation of the biasing magnetic field $\overline{H}_0^{(i)}$ and the sign of chirality parameters simultaneously. Also, (11) has no relation to the operating frequency and the geometrical parameters of the chiroferrite substrate, and it is also true for a chiroferrite superstrate-substrate structure. On the other hand, overall pattern resharping can easily be achieved by changing the biased field intensities as well as the orientation $(\varphi_0^{(i)}, \theta_0^{(i)})$ in each substrate layer.

Furthermore, Fig. 4 shows the effects of the azimuthal bias angles $\varphi_0^{(i)}$ of $\overline{H}_0^{(i)}$ on the main beam direction θ_m for a 13-layer chiroferrite substrate $(i = 1, \cdots, 13)$, and the operating frequency is assumed to be $f = 10$ GHz.

In Figs. 4(a)–(f), the orientations of the biasing magnetic fields $\overline{H}_0^{(i)}$ is kept in the x-y plane, and the phase difference $\Delta\varphi_0^{(i,i-1)} = \varphi_0^{(i)} - \varphi_0^{(i-1)}$ between two adjacent chiroferrite substrates is assumed to be 30° and 60°, respectively. Cases (a)(b)(d) and (e) correspond to the right-handed spirality, while (c) and (f) represent the left-handed spirality. Obviously, with $\varphi_0^{(i)}$ increasing, θ_m changes rapidly and sometimes continuously. Such phenomenon is mainly due to the strong variation of $\varphi_0^{(i)}$ in the z-direction. Under some circumstances, a beam scanning over large angles can be achieved only by adjusting the azimuthal angle $\varphi_0^{(i)}$. For example, in Figs. 4(a)(b)(c) the positive scanning angle of the main beam nearly is $+80^\circ$. Only reversing the orientation of $\overline{H}_0^{(i)}$ can also result in the change of θ_m in a wide range. When $\Delta\varphi_0^{(i,i-1)} = \pm 60^\circ$, very different tendencies are observed by comparison of (d)(e)(f) with (a)(b)(c). To some degree speaking, the scanning characteristics of the source are strongly governed by the phase difference $\Delta\varphi_0^{(i,i-1)}$. In addition, from (11) or numerical tests it is proven that the main beam direction θ_m satisfies the following relation:

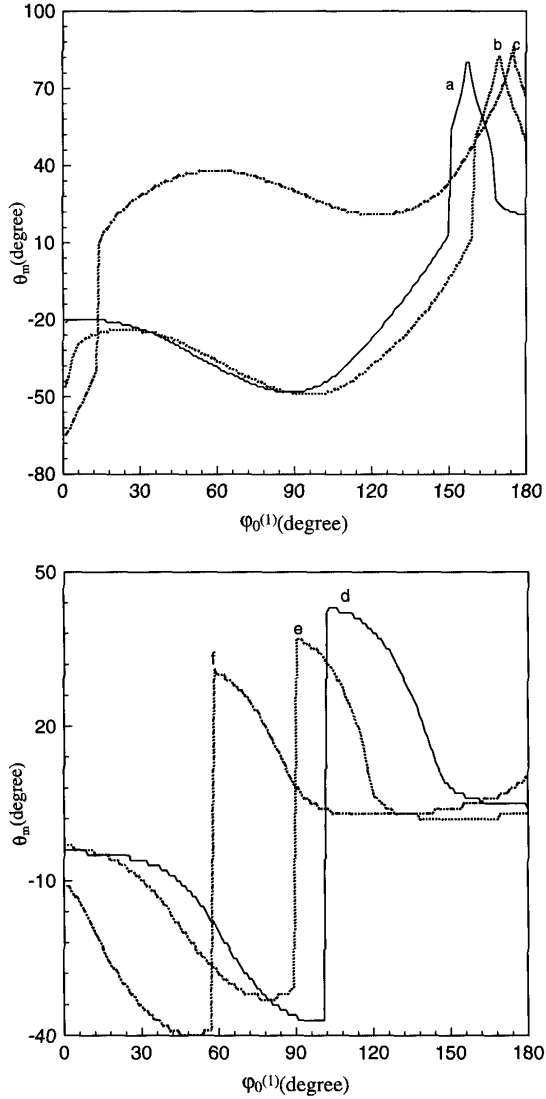

Figure 4. The main beam direction depending on the azimuthal bias angle $\varphi_0^{(i)}$ for a dipole antenna on a 13-layer chiroferrite substrate. $f = 10$ GHz, $\left[\varepsilon^{(i)}\right] = 12.6\overline{\overline{I}}$, $d^{(i)} = 0.2\,\text{mm}$, $\varphi = \theta_0^{(i)} = 90°$, $M_s^{(i)}\mu_0 = 0.275$, $\omega_0^{(i)}/\omega_m^{(i)} = 0.1$, and (a) $\kappa^{(i)} = 0.1$, $\varphi_0^{(i)} = \varphi_0^{(i-1)} + 30°(i = 1, \cdots, 13)$. (b) $\kappa^{(i)} = 0.4$, $\varphi_0^{(i)} = \varphi_0^{(i-1)} + 30°$. (c) $\kappa^{(i)} = 0.4$, $\varphi_0^{(i)} = \varphi_0^{(i-1)} - 30°$. (d) $\kappa^{(i)} = 0.1$, $\varphi_0^{(i)} = \varphi_0^{(i-1)} + 60°$. (e) $\kappa^{(i)} = 0.4$, $\varphi_0^{(i)} = \varphi_0^{(i-1)} + 60°$. (f) $\kappa^{(i)} = 0.4$, $\varphi_0^{(i)} = \varphi_0^{(i-1)} - 60°$.

$$\theta_m(\varphi, \theta_0^{(i)}, \pm\varphi_0^{(i)}, \pm\kappa^{(i)}) = \theta_m(180^\circ - \varphi, 180^\circ - \theta_0^{(i)}, \mp\varphi_0^{(i)}, \mp\kappa^{(i)}). \quad (12)$$

Fig. 5 depicts the main beam direction of a dipole antenna placed on a 13-layer chiroferrite substrate with increasing frequency. Since the magnitude of chirality parameter $\kappa^{(i)}$ used for calculation is small and the range of operating frequency is not too wide, the dispersion effect of $\kappa^{(i)}$ itself is neglected here.

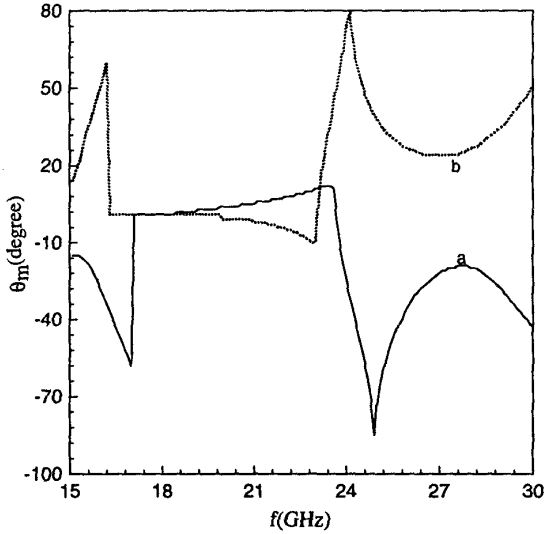

Figure 5. The main beam direction as a function of operating frequency for a dipole antenna on a 13-layer chiroferrite substrate. $[\varepsilon^{(i)}] = 15.1\overline{\overline{I}}$, $d^{(i)} = 0.2\,\text{mm}$, $\varphi = \theta_0^{(i)} = 90^\circ$, $M_s^{(i)}\mu_0 = 0.275$, $\omega_0^{(i)}/\omega_m^{(i)} = 0.1(i = 1, \cdots, 13)$, $\kappa^{(i)} = \pm 0.2$, (a) $\varphi_0^{(i)} = 0$. (b) $\varphi_0^{(i)} = \varphi_0^{(i-1)} \pm 60^\circ$.

In Fig. 5, it is assumed that the orientation of the biasing magnetic field $\overline{H}_0^{(i)}$ in each layer of the chirostrip substrate is kept in the x-direction in case (a), while for case (b), $\overline{H}_0^{(i)}$ is in the right- or left-handed spirality, respectively. Under this condition, nearly converse effects of the operating frequency on the main beam direction is observed, and it is further demonstrated that the right- or left-handed

orientation of $\overline{H}_0^{(i)}$ has significant effects on the main beam direction.

Finally, Fig. 6 shows the normalized far-field pattern of a dipole antenna on a 13-layer lossless chiroplasma substrate, and its geometrical size is chosen to be the same as above.

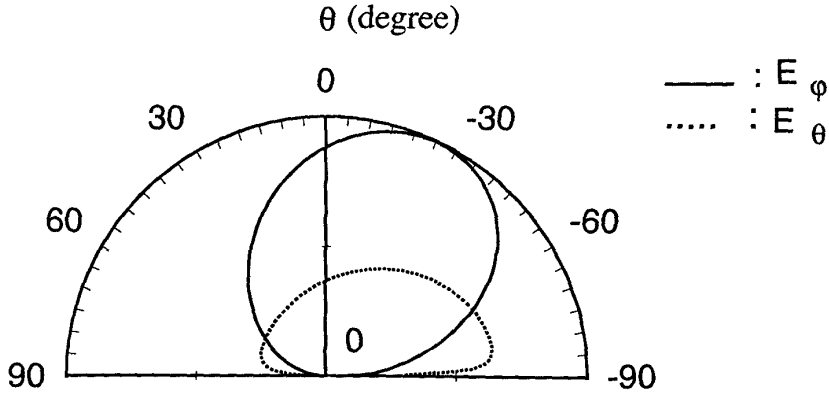

Figure 6. Normalized radiation pattern for a dipole antenna on a 13-layer chiroplasma substrate. $f = 17.25\,\text{GHz}$, $\varepsilon_s^{(i)} = 12.5$, $\left[\mu^{(i)}\right] = 1.0\overline{\overline{I}}$, $d^{(i)} = 0.2\,\text{mm}$, $\tau^{(i)} = 0$, $i = 1, \cdots, 13$, $\varphi = 90°$, $\omega_c^{(i)} = 2\omega_p^{(i)} = 1.5408 \times 10^{12}\,\text{rad/s}$, $\kappa^{(i)} = \pm 0.4$, $\theta_0^{(i)} = 90°$, $\varphi_0^{(i)} = 0°/\pm 60°/\pm 120°/\pm 180°/\pm 240°/\pm 300°/\pm 360°/\pm 60°/\pm 120°/\pm 180°/\pm 240°/\pm 300°/\pm 360°$.

In Fig. 6, the orientation of the external biasing DC magnetic field $\overline{B}_0^{(i)}$ is in the x-y plane and in the right- and left-handed spirality, respectively. So double chiralities are also introduced in the 13-layer chiroplasma substrate. The above described numerical investigation proves that

$$E_\varphi(\varphi, \pm\varphi_0^{(i)}, \pm\kappa^{(i)}) = E_\varphi(180° - \varphi, \mp\varphi_0^{(i)}, \mp\kappa^{(i)}), \tag{13a}$$

$$E_\theta(\varphi, \pm\varphi_0^{(i)}, \pm\kappa^{(i)}) = E_\theta(180° - \varphi, \mp\varphi_0^{(i)}, \mp\kappa^{(i)}), \tag{13b}$$

and the main beam direction

$$\theta_m(\varphi, \pm\varphi_0^{(i)}, \pm\kappa^{(i)}) = \theta_m(180° - \varphi, \mp\varphi_0^{(i)}, \mp\kappa^{(i)}). \tag{13c}$$

When $\theta_0^{(i)} \neq 90°$, (13) takes the general form of (11) and (12). A pattern resharping is also achievable here and in many different ways,

for instance, by changing the operating frequency, the geometrical size of substrate, the source place, the bias field strength as well as its right- or left-handed spiral orientation.

5. CONCLUSION

The generalized spectral-domain exponential matrix technique has been applied to examine the combined effects of chiral operations in multilayered bianisotropic substrate on the radiation characteristics of a dipole antenna, and the bianisotropic substrate is assumed to possess three different constitutive behaviors, respectively. Numerical investigations have been performed to demonstrate various influences of different constitutive and geometrical parameters of the substrate on the co- and cross-polarized far field components. Especially, some unique relations have been found corresponding to different chiral operations, which are also true for other cases of source excitation, such as infinite coupled dipole array, etc. It is believed that the present study can provide much insight into the physical characteristics of complex helicoidal bianisotropic composites.

ACKNOWLEDGMENT

W. Y. Yin appreciates the Alexander von Humboldt Research Foundation of Germany greatly for its sponsorship of this research, and G. H. Nan is supported by the scholarship of German Academic Exchange Service (DAAD).

APPENDIX 1:

In (7),

$$\begin{aligned} p_{11}^{(i)} =& - jk_0 \left\{ \eta_{yx}^{(i)} + \frac{1}{D^{(i)}} \{ Q_1^{(i)} [\varepsilon_{zx}^{(i)} \mu_{zz}^{(i)} - \xi_{zz}^{(i)} (\eta_{zx}^{(i)} + k_{y0})] \right. \\ & \left. - \mu_{yz}^{(i)} (\varepsilon_{zz}^{(i)} \eta_{zx}^{(i)} + \varepsilon_{zz}^{(i)} k_{y0} - \varepsilon_{zx}^{(i)} \eta_{zz}^{(i)}) \} \right\}, \\ p_{12}^{(i)} =& - jk_0 \left\{ \eta_{yy}^{(i)} + \frac{1}{D^{(i)}} \{ Q_1^{(i)} [\varepsilon_{zy}^{(i)} \mu_{zz}^{(i)} - \xi_{zz}^{(i)} (\eta_{zy}^{(i)} - k_{x0})] \right. \\ & \left. - \mu_{yz}^{(i)} (\varepsilon_{zz}^{(i)} \eta_{zy}^{(i)} - \varepsilon_{zz}^{(i)} k_{x0} - \varepsilon_{zy}^{(i)} \eta_{zz}^{(i)}) \} \right\}, \\ p_{13}^{(i)} =& - jk_0 \eta_0 \left\{ \mu_{yx}^{(i)} + \frac{1}{D^{(i)}} \{ Q_1^{(i)} [\mu_{zz}^{(i)} (\xi_{zx}^{(i)} - k_{y0}) - \xi_{zz}^{(i)} \mu_{zx}^{(i)}] \right. \end{aligned}$$

$$
\begin{aligned}
&-\mu_{yz}^{(i)}[\varepsilon_{zz}^{(i)}\mu_{zx}^{(i)}-\eta_{zz}^{(i)}(\xi_{zx}^{(i)}-k_{y0})]\}\Big\},\\
p_{14}^{(i)}=&-jk_0\eta_0\Big\{\mu_{yy}^{(i)}+\frac{1}{D^{(i)}}\{Q_1^{(i)}[\mu_{zz}^{(i)}(\xi_{zy}^{(i)}+k_{x0})-\xi_{zz}^{(i)}\mu_{zy}^{(i)}]\\
&-\mu_{yz}^{(i)}[\varepsilon_{zz}^{(i)}\mu_{zy}^{(i)}-\eta_{zz}^{(i)}(\xi_{zy}^{(i)}+k_{x0})]\}\Big\},\\
p_{21}^{(i)}=&jk_0\Big\{\eta_{xx}^{(i)}+\frac{1}{D^{(i)}}\{Q_2^{(i)}[\varepsilon_{zx}^{(i)}\mu_{zz}^{(i)}-\xi_{zz}^{(i)}(\eta_{zx}^{(i)}+k_{y0})]\\
&-\mu_{xz}^{(i)}(\varepsilon_{zz}^{(i)}\eta_{zx}^{(i)}+\varepsilon_{zz}^{(i)}k_{y0}-\varepsilon_{zx}^{(i)}\eta_{zz}^{(i)})\}\Big\},\\
p_{22}^{(i)}=&jk_0\Big\{\eta_{xy}^{(i)}+\frac{1}{D^{(i)}}\{Q_2^{(i)}[\varepsilon_{zy}^{(i)}\mu_{zz}^{(i)}-\xi_{zz}^{(i)}(\eta_{zy}^{(i)}-k_{x0})]\\
&-\mu_{xz}^{(i)}(\varepsilon_{zz}^{(i)}\eta_{zy}^{(i)}-\varepsilon_{zz}^{(i)}k_{x0}-\varepsilon_{zy}^{(i)}\eta_{zz}^{(i)})\}\Big\},\\
p_{23}^{(i)}=&jk_0\eta_0\Big\{\mu_{xx}^{(i)}+\frac{1}{D^{(i)}}\{Q_2^{(i)}[\mu_{zz}^{(i)}(\xi_{zx}^{(i)}-k_{y0})-\xi_{zz}^{(i)}\mu_{zx}^{(i)}]\\
&-\mu_{xz}^{(i)}[\varepsilon_{zz}^{(i)}\mu_{zx}^{(i)}-\eta_{zz}^{(i)}(\xi_{zx}^{(i)}-k_{y0})]\}\Big\},\\
p_{24}^{(i)}=&jk_0\eta_0\Big\{\mu_{xy}^{(i)}+\frac{1}{D^{(i)}}\{Q_2^{(i)}[\mu_{zz}^{(i)}(\xi_{zy}^{(i)}+k_{x0})-\xi_{zz}^{(i)}\mu_{zy}^{(i)}]\\
&-\mu_{xz}^{(i)}[\varepsilon_{zz}^{(i)}\mu_{zy}^{(i)}-\eta_{zz}^{(i)}(\xi_{zy}^{(i)}+k_{x0})]\}\Big\},\\
p_{31}^{(i)}=&jk_0\Big\{\varepsilon_{yx}^{(i)}+\frac{1}{D^{(i)}}\{Q_3^{(i)}[\varepsilon_{zz}^{(i)}(-\eta_{zx}^{(i)}-k_{y0})+\eta_{zz}^{(i)}\varepsilon_{zx}^{(i)}]\\
&-\varepsilon_{yz}^{(i)}[\mu_{zz}^{(i)}\varepsilon_{zx}^{(i)}+\xi_{zz}^{(i)}(-\eta_{zx}^{(i)}-k_{y0})]\}\Big\}/\eta_0,\\
p_{32}^{(i)}=&jk_0\Big\{\varepsilon_{yy}^{(i)}+\frac{1}{D^{(i)}}\{Q_3^{(i)}[\varepsilon_{zz}^{(i)}(-\eta_{zy}^{(i)}+k_{x0})+\eta_{zz}^{(i)}\varepsilon_{zy}^{(i)}]\\
&-\varepsilon_{yz}^{(i)}[\mu_{zz}^{(i)}\varepsilon_{zy}^{(i)}+\xi_{zz}^{(i)}(-\eta_{zy}^{(i)}+k_{x0})]\}\Big\}/\eta_0,\\
p_{33}^{(i)}=&-jk_0\Big\{-\xi_{yx}^{(i)}+\frac{1}{D^{(i)}}\{Q_3^{(i)}[\mu_{zx}^{(i)}\varepsilon_{zz}^{(i)}+\eta_{zz}^{(i)}(-\xi_{zx}^{(i)}+k_{y0})]\\
&-\varepsilon_{yz}^{(i)}(-\mu_{zz}^{(i)}\xi_{zx}^{(i)}+\mu_{zz}^{(i)}k_{y0}+\mu_{zx}^{(i)}\xi_{zz}^{(i)})\}\Big\},\\
p_{34}^{(i)}=&-jk_0\Big\{-\xi_{yy}^{(i)}+\frac{1}{D^{(i)}}\{Q_3^{(i)}[\mu_{zy}^{(i)}\varepsilon_{zz}^{(i)}+\eta_{zz}^{(i)}(-\eta_{zy}^{(i)}-k_{x0})]\\
&-\varepsilon_{yz}^{(i)}(-\mu_{zz}^{(i)}\xi_{zy}^{(i)}-\mu_{zz}^{(i)}k_{x0}+\mu_{zy}^{(i)}\xi_{zz}^{(i)})\}\Big\},
\end{aligned}
$$

$$
\begin{aligned}
p_{41}^{(i)} =& - jk_0 \left\{ \varepsilon_{xx}^{(i)} + \frac{1}{D^{(i)}} \{ Q_4^{(i)} [\varepsilon_{zz}^{(i)} (-\eta_{zx}^{(i)} - k_{y0}) + \eta_{zz}^{(i)} \varepsilon_{zx}^{(i)}] \right. \\
& \left. - \varepsilon_{xz}^{(i)} [\mu_{zz}^{(i)} \varepsilon_{zx}^{(i)} + \eta_{zz}^{(i)} (-\xi_{zx}^{(i)} - k_{y0})] \} \right\} / \eta_0, \\
p_{42}^{(i)} =& - jk_0 \left\{ \varepsilon_{xy}^{(i)} + \frac{1}{D^{(i)}} \{ Q_4^{(i)} [\varepsilon_{zz}^{(i)} (-\eta_{zy}^{(i)} + k_{x0}) + \eta_{zz}^{(i)} \varepsilon_{zy}^{(i)}] \right. \\
& \left. - \varepsilon_{xz}^{(i)} [\mu_{zz}^{(i)} \varepsilon_{zy}^{(i)} + \xi_{zz}^{(i)} (-\eta_{zy}^{(i)} + k_{x0})] \} \right\} / \eta_0, \\
p_{43}^{(i)} =& jk_0 \left\{ -\xi_{xx}^{(i)} + \frac{1}{D^{(i)}} \{ Q_4^{(i)} [\mu_{zx}^{(i)} \varepsilon_{zz}^{(i)} + \eta_{zz}^{(i)} (-\xi_{zx}^{(i)} + k_{y0})] \right. \\
& \left. - \varepsilon_{xz}^{(i)} (-\mu_{zz}^{(i)} \xi_{zx}^{(i)} + \mu_{zz}^{(i)} k_{y0} + \mu_{zx}^{(i)} \xi_{zz}^{(i)}) \} \right\}, \\
p_{44}^{(i)} =& jk_0 \left\{ -\xi_{xy}^{(i)} + \frac{1}{D^{(i)}} \{ Q_4^{(i)} [\mu_{zy}^{(i)} \varepsilon_{zz}^{(i)} + \eta_{zz}^{(i)} (-\xi_{zy}^{(i)} - k_{x0})] \right. \\
& \left. - \varepsilon_{xz}^{(i)} (-\mu_{zz}^{(i)} \xi_{zy}^{(i)} - \mu_{zz}^{(i)} k_{x0} + \mu_{zy}^{(i)} \xi_{zz}^{(i)}) \} \right\}, \qquad \text{(A1)}
\end{aligned}
$$

where $k_{x0} = k_x/k_0$, $k_{y0} = k_y/k_0$, $k_0 = \omega\sqrt{\mu_0\varepsilon_0}$, $Q_1^{(i)} = -k_{x0} - \eta_{yz}^{(i)}$, $Q_2^{(i)} = -k_{y0} - \eta_{xz}^{(i)}$, $Q_3^{(i)} = -k_{x0} + \xi_{yz}^{(i)}$, $Q_4^{(i)} = -k_{y0} + \xi_{xz}^{(i)}$, $D^{(i)} = \varepsilon_{zz}^{(i)} \mu_{zz}^{(i)} - \xi_{zz}^{(i)} \eta_{zz}^{(i)}$.

REFERENCES

1. Graglia, R. D., P. L. E. Uslenghi, and R. E. Zich, "Dispersion relation for bianisotropic materials and its symmetry properties," *IEEE Trans. Antennas Propagat.*, Vol. 39, No. 1, 83–90, 1991.
2. Mesa, F. L., R. Marques, and M. Horno, "A generalized algorithm for computing the bidimensional spectral Green's dyad in multilayered complex bianisotropic media: the equivalent boundary method," *IEEE Trans. Microwave Theory Tech.*, Vol. 39, No. 9, 1640–1648, 1991.
3. Tsalamengas, J. L., "Interaction of electromagnetic waves with general bianisotropic slabs," *IEEE Trans. Microwave Theory and Tech.*, Vol. 40, No. 10, 1870–1878, 1992.
4. Olyslager, F., "Time-harmonic two- and three-dimensional Green's dyadics for general uniaxial bianisotropic media," *IEEE Trans. Antennas and Propagat.*, Vol. 43, No. 4, 430–434, 1995.
5. Olyslager, F., and B. Jakoby, "Time- harmonic two- and three-dimensional Green's dyadics for a special class of gyrotropic bianisotropic media," *IEE Proc.-Microw. Antennas and Propagat.*, Vol. 143, No. 5, 413–416, 1996.

6. Weiglhofer, W. S., and A. Lakhtakia, "Dyadic Green functions for axially varying fields in helicoidal bianisotropic media," *J. Appl. Electromagn. Mech.*, Vol. 6, 221–234, 1995.
7. Lakhtakia, A., and W. S. Weiglhofer, "Green function for radiation and propagation in helicoidal bianisotropic mediums," *IEE Proc.-H*, Vol. 144, No. 1, 55–59, 1997.
8. Lakhtakia, A., K. Robbie, and M. J. Brett, "Spectral Green's function for wave excitation and propagation in a piezoelectric, continuously twisted, structurally chiral medium," *J. Acoust. Soc. Am.*, Vol. 101, No. 4, 2052–2058, 1997.
9. Lakhtakia, A., and W. S. Weiglhofer, "On light propagation in helicoidal bianisotropic medium," *Proc. R. Soc. Lond. A*, Vol. 438, 419–437, 1995.
10. Lakhtakia, A., "Wave propagation in a piezoelectric continuously twisted, structurally chiral medium along the axis of spirality," *Appl. Acoust.*, Vol. 44, 25–37, 1995; errata: Vol. 44, 385, 1995.
11. Lakhtakia, A., and W. S. Weiglhofer, "Further results on light propagation in helicoidal bianisotropic mediums: oblique propagation," *Proc. R. Soc. Lond.*, A, 453, 93–105, 1997.
12. Lakhtakia, A., "Exact analytic solution for oblique propagation in a piezoelectric, continuously twisted, structurally chiral medium," *Appl. Acoust.*, Vol. 49, 222–236, 1996.
13. He, S., and I. V. Lindell, "Propagation eigenmodes for plane waves in a uniaxial bianisotropic medium and reflection from a planar interface," *IEEE Trans. Antennas Propagat.*, Vol. 41, No. 12, 1659–1664, 1993.
14. Yang, H.-Y., "A spectral recursive transmission method for electromagnetic waves in generalied anisotropic layered media," *IEEE Trans. Antennas Propagat.*, Vol. 45, No. 3, 520–526, 1997.
15. Norgren, M., and S. He, "On the possibility of reflectionless coating of a homogeneous bianisotropic layer on a perfect conductor," *Electromagnetics,* Vol. l7, No. 4, 295–308, 1997.
16. Yang, H.-Y., and P. L. E. Uslenghi, "Theory of certain bianisotropic waveguide," *Radio Science*, Vol. 28, 919–927, 1993.
17. Olyslager, F., "Properties of and generalized full- wave transmission line models for hybrid (bi)(an)isotropic waveguides," *IEEE Trans. Microwave Theory Tech.*, Vol. 44, No. 11, 2064–2075, 1996.
18. Graglia, R. D., M. S. Sarto, and P. L. E. Uslenghi, "TE and TM modes in cylindrical metallic structures filled with bianisotropic materials," *IEEE Trans. Microwave Theory Tech.*, Vol. 44, No. 8, 1470–1477, 1996.

19. Uslenghi, P. L. E, "TE-TM decoupling for guided propagation in bianisotropic media," *IEEE Trans. Antennas Propagat.*, Vol. 45, No. 2, 284–286, 1997.
20. Xu, Y., and R. G. Bosisio, "An efficient method for study of general bianisotropic waveguides," *IEEE Trans. Microwave Theory Tech.*, Vol. 43, No. 4, 873–879, 1995.
21. Xu, Y., and R. G. Bosisio, "A study on the solutions of chirowaveguides bianisotropic waveguides with the use of coupled-mode analysis," *Micro. Opt. Tech. Lett.*, Vol. 14, No. 5, 308–311, 1997.
22. Valor, L., and J. Zapata, "An efficient finite element formulation to analyze waveguides with lossy inhomogeneous bianisotropic materials," *IEEE Trans. Microwave Theory Tech.*, Vol. 44, No. 2, 291–296, 1996.
23. Jakoby, B., and D. D. Zutter, "Analysis of guided waves in inhomogeneous bianisotropic cylindrical waveguides," *IEEE Trans. Microwave Theory Tech.*, Vol. 44, No. 2, 297–310, 1996.
24. Yin, W. Y., W. Wan, and W. B. Wang, "'Mode bifurcation and attenuation in circular Faraday chirowaveguide-summary," *J. Electromagn. Waves and Appl.*, Vol. 10, 1389–1394, 1996.
25. Olyslager, F., E. Laermans, and D. D. Zutter,"Rigorous quasi-TEM analysis of multiconductor transmission lines in bi-isotropic media- Part I: theoretical analysis for general inhomogeneous media and generalization to bianisotropic media," *IEEE Trans. Microwave Theory Tech.*, Vol. 43, No. 7, 1409–1415, 1995.
26. Jakoby, B., and Ali-Reza Baghai-Wadji, "Analysis of bianisotropic layered structures with laterally periodic inhomogeneities– an eigenoperator formulation," *IEEE Trans. Antennas Propagat.*, Vol. 44, No. 5, 615–626, 1996.
27. Hanson, G. W., "A numerical formulation of dyadic Green's functions for planar bianisotropic media with application to printed transmission lines," *IEEE Trans. Microwave Theory Tech.*, Vol. 44, No. 1, 144–151, 1996.
28. Yin, W. Y., W. Wan, and W. B. Wang, "Radiation from a dipole antenna on two-layer grounded Faraday chiral substrates," *J. Electromagn. Waves and Appl.*, Vol. 9, No. 7/8, 1027–1044, 1995.
29. Yin, W. Y., "The features of Mueller scattering scattering matrix for two penetrable composite Faraday chiral cylinder," *J. Electromagn. Waves and Appl.*, Vol. 10, 1199–1216, 1996.
30. Yin, W. Y., H. L. Zhao, and W. Wan, "Parametric study on the scattering characteristics of two impedance cylinders eccentrically coated with Faraday chiral materials," *J. Electromagn. Waves and Appl.*, Vol. 10, 1467–1484, 1996.

31. Yin, W. Y., "Scattering by a linear array of uniaxial bianisotropic chiral cylinders," *Micro. and Opt. Tech. Lett.*, Vol. 12, No. 5, 287–295, 1996.
32. Olyslager, F., "The behavior of electromagnetic fields at edges in bi-isotropic and bianisotropic materials," *IEEE Trans. Antennas Propagat.*, Vol. 42, No. 10, 1392–1397, 1994.
33. Olyslager, F., "Overview of the singular behavior of electromagnetic fields at edges and tips in bi-isotropic and special bianisotropic media," *Radio Science*, Vol. 30, No. 5, 1349–1354, 1995.
34. Sihvola, A. H., J. O. Juntunen, and P. Eratuuli, "Macroscopic electromagnetic properties of bi-anisotropic mixtures," *IEEE Trans. Antennas Propagat.*, Vol. 44, No. 6, 836–843, 1996.
35. Chung, C. Y., and K. W. Whites, "Effective constitutive parameters for an artificial uniaxial bianisotropic chiral medium," *J. Electromagn. Waves and Appl.*, Vol. 10, 1363–1388, 1996.
36. Whites, K. W., and C. Y. Chung, "Composite uniaxial bianisotropic chiral materials characterization: comparison of predicted and measured scattering," *J. Electromagn. Waves and Appl.*, Vol. 11, 377–387, 1997.
37. Theron, I. P., and J. H. Cloete, "The electric quadrupole contribution to the circular birefringence of nonmagnetic anisotropic chiral media: a circular waveguide experiment," *IEEE Trans. Microwave Theory Tech.*, Vol. 44, No. 4, 1451–1459, 1996.
38. Kamenetskii, E. O., "On the technology of making chiral and bianisotropic waveguides for microwave propagation," *Micro. Opt. Tech. Lett.*, Vol. 14, No. 11, 103–107, 1996.
39. Tretyakov, S. A., A. A. Sochava, and D. Y. Khaliullin, "Artificial nonreciprocal uniaxial magnetoelectric composites," *Micro. Opt. Tech. Lett.*, Vol. 15, No. 4, 260–263, 1997.
40. Varadan, V. V., A. Lakhtakia, and V. K. Varadan, "Propagation through a periodic chiral arrangement of identical uniaxial dielectric layers and its effective properties," *Optik*, Vol. 83, No. 1, 26–29, 1989.
41. Kazantsev, Y. N., and G. A. Kraftmakher, "Microwave permeability of chiral media. Mutual influence of chiral and ferromagnetic resonances in a chiral medium-ferrite structure," *J. Commun. Tech. and Electron.*, Vol. 42, No. 3, 277–283, 1997.
42. Taouk, H., "Optical wave propagation in active media: Gyrotropic-gyrochiral media," *J. Opt. Soc. Am. A*, Vol. 14, No. 3, 193–200, 1997.

43. Mesa, F., and M. Horno, "Application of the spectral domain method for the study of surface slow waves in nonreciprocal planar structures with a multilayered gyroelectric substrate," *IEE Proc.-H*, Vol. 140, No. 3, 193–200, 1993.
44. Hsia, I. Y., and N. G. Alexopoulos, "Radiation characteristics of Hertzian dipole antennas in a nonreciprocal superstrate-substrate structure," *IEEE Trans. Antennas Propagat.*, Vol. 40, No. 7, 782–790, 1992.
45. Yang, H.-Y., J. A. Castaneda, and N. G. Alexopoulos, "Infinite phased arrays of microstrip antennas on generalized anisotropic substrate," *Electromagnetics*, Vol. 11, No. 1, 107–124, 1991.